

# Conductance of Connexin Hemichannels Segregates with the First Transmembrane Segment

Xinge Hu, Meiyun Ma, and Gerhard Dahl

Department of Physiology and Biophysics, University of Miami, School of Medicine, Miami, Florida 33101

**ABSTRACT** Gap junction channels are intercellular channels that mediate the gated transfer of molecules between adjacent cells. To identify the domain determining channel conductance, the first transmembrane segment (M1) was reciprocally exchanged between Cx46 and Cx32E<sub>1</sub>43. The resulting chimeras exhibited conductances similar to that of the respective M1 donor. Furthermore, a chimera with the carboxy-terminal half of M1 in Cx46 replaced by that of Cx32 exhibited a conductance similar to that of Cx32E<sub>1</sub>43, whereas the chimera with only the amino-terminal half of M1 replaced retained the unitary conductance of wild-type Cx46. Extending the M1 domain swapping to other connexins by replacing the carboxy-terminal half of M1 in Cx46 with that of Cx37 yielded a chimera channel with increased unitary conductance close to that of Cx37. Furthermore, a point mutant of Cx46, with leucine substituted by glycine in position 35, displayed a conductance much larger than that of the wild type. Thus, the M1 segment, especially the second half, contains important determinants of conductance of the connexin channel.

## INTRODUCTION

Gap junctions contain intercellular channels that are found in almost all multicellular organisms. In vertebrates they are found in all tissues except mature blood cells and mature skeletal muscles (1,2). They provide a hydrophilic path that allows the passage of molecules up to 0.8–1.4 nm in size and 1000 Da in molecular mass. Gap junction channels are formed by two hemichannels docking to each other. Each hemichannel is composed of six subunits, connexins in vertebrates and innexins in invertebrates. Recently a new family of gap junction proteins with sequence homology to innexins was identified in vertebrates. They are named pannexins (3,4). At least 21 connexins and three pannexins have been identified in the human genome (5,6). The distribution of connexins is tissue specific and the pattern of distribution is conserved among different species. Gap junction channels formed by different connexins display distinct conductance, permeability, and gating properties (7,8). Different connexins cannot be functionally substituted for one another as demonstrated by diverse disease causing connexin mutations as well as knock-out/knock-in mutations in mice (9), underscoring the unique property of each connexin with respect to distribution, conductance, and permeability, etc. that are at the root of their tissue-specific functions.

Typically gap junction hemichannels (connexons) are closed under physiological conditions. Exceptions are the lens connexins, Cx46 and Cx50, and the mutant Cx32E<sub>1</sub>43 when these are expressed in *Xenopus* oocytes (10–12). Cx32E<sub>1</sub>43, is a chimera in which the first extracellular loop of Cx32 is replaced by the corresponding Cx43 sequence.

Connexons that function as open hemichannels are also observed in cultured retinal horizontal cells, astrocytes, and ventricular myocytes, etc. under special experimental conditions (13–15). The conductance of the hemichannels is twice the conductance of complete gap junction channels, as if gap junctions form by pairing of two hemichannels in series without apparent pore structure changes following the docking process. Like complete gap junction channels, open hemichannels are gated by voltage, as well as intracellular acidification and elevated Ca<sup>2+</sup> concentration (16–19). Open hemichannels, thus, are a valuable tool that allows addressing the fundamental properties of the connexin channel, for example the permeation pore, in a more direct way.

The membrane topology of connexin channels is well characterized. The connexins have four membrane-spanning segments (M1–M4), one cytoplasmic loop, and two extracellular loops (E1 and E2). However, the functional domains determining channel permeability are poorly identified. Application of substituted cysteine accessibility method (SCAM) (20) on open hemichannels indicated that both M1 and perhaps M3 contain potential pore lining residues because of the existence of reactive cysteine sites in these two segments (21–23). Reactivity was found to extend into positions in the first extracellular loop, which is logical, as the gap junction channel spans the extracellular space (22). Recent crystallographic data appear to confirm the contributions of M1 and M3 to the pore lining (24). However, SCAM on Cx32 gap junctions in paired oocytes with the cut-open method yielded a multitude of reactive sites with every transmembrane segment represented (25). Several reasons could account for this discrepancy.

In a previous study we used an independent approach, the exchange of domains between connexins, to test the involvement of M1 in pore formation (26). Domain swapping

Submitted May 11, 2005, and accepted for publication September 13, 2005.

Address reprint requests to Gerhard Dahl, University of Miami School of Medicine, Dept. of Physiology and Biophysics, 1600 NW 10th Ave., Miami, FL 33136. Tel.: 305-243-5776; Fax: 305-243-5931; E-mail: gdahl@miami.edu.

© 2006 by the Biophysical Society

0006-3495/06/01/140/11 \$2.00

doi: 10.1529/biophysj.105.066373

mutagenesis has been successfully applied to a number of channels to identify pore domains (27–30). The large conductance of Cx46 indeed was conferred to Cx32E<sub>1</sub>43 by inserting the Cx46 M1 sequence into Cx32E<sub>1</sub>43. However, the transfer of conductance could have been fortuitous. Furthermore, the presence of a foreign M1 sequence in a connexin does not necessarily result in transfer of conductance as observed in a different context of domain exchange (28). In addition, channel conductance can be affected by mutations in various parts of the molecule including the carboxy-terminus (28,31,32). In this article we refine the domain exchange approach by studying reciprocal exchanges and extend the exchanges to a connexin with higher conductance, Cx37.

## MATERIALS AND METHODS

### Construction of mutants

Construction of Cx32M<sub>1</sub>46 E<sub>1</sub>43 was described previously (26). Cx46 was obtained from Dr. D. Paul (10). Other mutants were constructed by the following procedure (Fig. 1). For Cx46M<sub>1</sub>32I, the replacement cassette was prepared by polymerase chain reaction (PCR) with the primers: I, ggccacgatgctccggcgtagagg, II, gtgtgctgagcgtcatcttcatctccg, III, cggaagatgaagatgacgctcagccacac, and IV, ctccccgtctttcttctctccc, and with Cx46 as templates. This yielded the insertion cassette with a new restriction site by *Bln*I. Primer I and IV for Cx46M<sub>1</sub>32II, Cx46L35G, and Cx46M<sub>1</sub>37 were the same as for Cx46M<sub>1</sub>32I. Primer II and III for Cx46M<sub>1</sub>32II were cgcattatgctgctggtt ggctgcagaggag and ctctctgcagccaccaccagcaccataatgcg, respectively. Primer II and III for Cx46L35G were catctccgcattggcgtcctagggcggc and cgcccctaggacccaatgcggaagatg, respectively. For Cx46M<sub>1</sub>37, primer II and primer III were gcattctgattctgggctggcagggcaggaggtgtgg and ccacacctctgcctccagcccccagaatcagaatgc, respectively. The newly introduced restriction site was *Pst*I for Cx46M<sub>1</sub>32II, *Avr*II for Cx46L35G, and *Hin*I for Cx46M<sub>1</sub>37. Cx46M<sub>1</sub>32 were prepared by using Cx46M<sub>1</sub>32II as templates and primers for Cx46M<sub>1</sub>32I as primers. After digestion with *Nhe*I and *Pml*I the cassette was inserted into Cx46 containing vector cut with the same enzymes. All mutants were selected by screening test using specific restriction enzyme and confirmed by DNA sequencing.

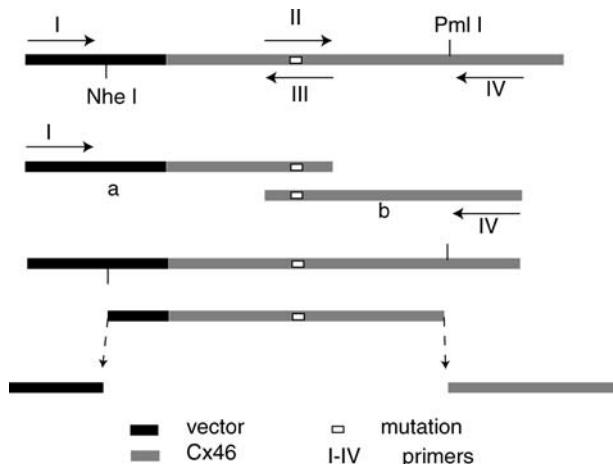


FIGURE 1 Construction of the Cx46 mutants: Cx46M<sub>1</sub>32, Cx46M<sub>1</sub>37, and Cx46L35G. A replacement cassette flanked by two restriction enzyme sites, *Nhe*I and *Pml*I, was generated by PCR.

### Expression of mRNA in oocytes

Synthetic mRNA was prepared using the mMESSAGEMACHINE transcription kit (Ambion, Austin, TX). Oocytes were prepared as described earlier (33) and stored in OR<sub>2</sub> solution (82.5 mM NaCl, 2.5 mM KCl, 1.0 mM MgCl<sub>2</sub>, 1.0 mM CaCl<sub>2</sub>, 1.0 mM Na<sub>2</sub>HPO<sub>4</sub>, and 5.0 mM HEPES, pH 7.5) at 18°C; 20 nl mRNA (50 ng/μl) was injected into oocytes. The injected oocytes were then stored in high Ca<sup>2+</sup> (5 mM) OR<sub>2</sub> solution to keep the hemichannel closed. Oocytes injected with various connexins were tested by whole-cell voltage clamp to determine expression levels. The oocytes were transferred back to regular OR<sub>2</sub> solution before electrophysiological recordings.

### Patch-clamp recording

The vitelline membrane of the oocytes was removed. If not specified, both bath and pipette solutions were potassium gluconate solution (140 mM Kglu, 10 mM KCl, and 5.0 mM TES, pH 7.5). Electrode pipettes (OD, 1.5 mm, ID, 0.86 mm; Warner Instruments, Hamden, CT) were pulled by Flaming-Brown micropipette puller (Sutter Instrument, Novato, CA) and polished by microforge (Narishige Scientific Instrument, Tokyo, Japan) to 0.5–1 μm with a resistance of 10–20 MΩ in Kglu solution. Single connexin hemichannels were studied by patch-clamp technique (23,34) using an Axopatch-1B amplifier (Axon Instruments, Inverurie, Scotland, UK). Excised inside-out and outside-out patches were used. All recordings were filtered at 5 kHz, digitized using a VR-10B digital data recorder, and stored on videotape. The recordings were transferred to a Power Macintosh (Apple, Cupertino, CA) and data were analyzed by TAC software (Bruxon, Seattle, WA).

## RESULTS

### Transfer of single-channel conductance by exchange of the first transmembrane segment (M1) between Cx46 and Cx32E<sub>1</sub>43

A few connexins form open hemichannels without docking under physiological conditions. These open hemichannels share most of the properties of complete gap junction channels. The resistance of a hemichannel is about half of the junctional channel, which can be explained by pairing two hemichannels in series without apparent structural change of the permeation pathway by the docking process. In this article we make use of two connexins that can form functional hemichannels when expressed in oocytes. One is Cx46. The other is Cx32E<sub>1</sub>43, a chimera with E1 in Cx32 replaced by the corresponding sequence of Cx43.

Sequence alignment of M1 identifies five amino acids differing between Cx46 and Cx32E<sub>1</sub>43, three of which are located toward the extracellular end of M1 (Fig. 2). Cx46 and Cx32E<sub>1</sub>43 can be easily distinguished from each other due to a large difference in single-channel conductance and gating kinetics (26). The single-channel conductance of Cx46 was 270 pS at –30 mV (Fig. 3 a) and 120 pS at +30 mV (Fig. 4 a). The opening and closing of Cx46 channels were relative slow and in a stepwise manner. At positive potential Cx46 channels preferred to stay in a subconductance state, which was approximately one-third of the maximal conductance (Fig. 4 a). In contrast, the single channel conductance of Cx32E<sub>1</sub>43 was 50 pS at –30 mV (Fig. 3 b) and 30 pS at +30 mV (Fig. 4 b). The opening and closing of Cx32E<sub>1</sub>43

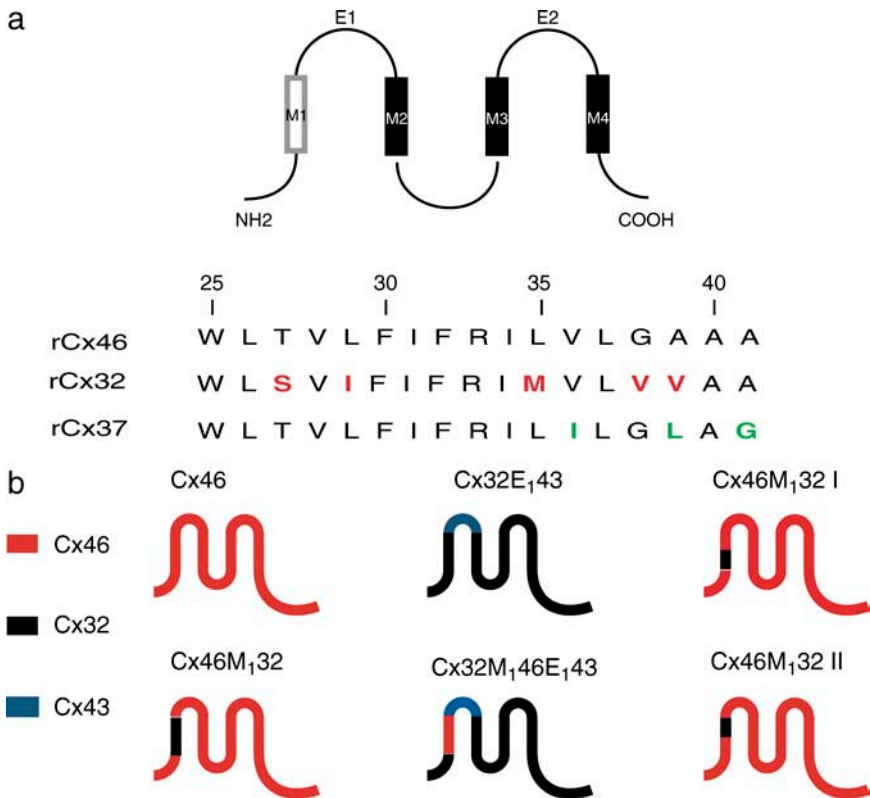


**FIGURE 2** (a) Membrane topology of connexins and sequence alignment of the M1 segment between Cx46, Cx32, and Cx37. Sequence alignment identifies five-amino-acids difference between Cx46 and Cx32 (red), and three-amino-acids difference between Cx46 and Cx37 (green). (b) Summary of chimeras.

channel was fast and the open times brief. At positive potential no obvious subconductance state was observed in the Cx32E<sub>1</sub>43 channel (Fig. 4 b). Thus, Cx46 and Cx32E<sub>1</sub>43 differ in not only single-channel conductance but also channel kinetics as well as gating properties.

One chimera, Cx32M<sub>1</sub>46E<sub>1</sub>43 with M1 derived from Cx46, exhibited single-channel activities similar to Cx46. The unitary conductance of Cx32M<sub>1</sub>46E<sub>1</sub>43 was 260 pS at -30 mV (Fig. 3 c) and 225 pS at +40 mV (Fig. 4 c). The opening and closing transitions of Cx32M<sub>1</sub>46E<sub>1</sub>43 were slow. At positive potentials Cx32M<sub>1</sub>46E<sub>1</sub>43 channels dwelled mainly in a subconductance state, which was about one-third of the maximal conductance (Fig. 4 c).

The chimera Cx46M<sub>1</sub>32, with M1 derived from Cx32 exhibited single-channel properties similar to Cx32E<sub>1</sub>43. The single-channel conductance of Cx46M<sub>1</sub>32 was 50 pS at -30 mV (Fig. 3 d) and 46 pS at +30 mV (Fig. 4 d). The transitions between closed and open state were fast. At positive potential, the channel mainly flickered between fully closed and open states (Fig. 4 d). Thus, the above two chimeras acquired properties of single-channel conductance, channel kinetics, and preference to dwelling in a subconductance state from the M1 donor in response to M1 exchange. Cx46 and Cx32E<sub>1</sub>43 channel rectified at positive potentials. Rectification of channel current was not as pronounced in the chimeras (supplement Fig. 1).

To further localize the determinants of channel conductance, we divided the M1 segment of Cx32 into two halves. Each

half was used to substitute the correspondent part on Cx46. This yielded the chimeras Cx46M<sub>1</sub>32I and Cx46M<sub>1</sub>32II. Cx46M<sub>1</sub>32I, with only the cytoplasmic half of M1 in Cx46 replaced by that of Cx32, exhibited channel properties similar to Cx46 (Figs. 3 e and 4 e). The single-channel conductance was ~270 pS at -30 mV. The channel dwelled in a subconductance state at positive potentials. In contrast, Cx46M<sub>1</sub>32II, with replacement of the extracellular half of M1, exhibited channel conductance similar to Cx32E<sub>1</sub>43 (Figs. 3 f and 4 f), ~50 pS at -30 mV. There was no obvious subconductance state observed at positive potentials. Thus, the swapping of the intracellular half of M1 alone did not change channel conductance and gating properties, whereas replacing the extracellular half of M1 changed channel properties to the same extent as if the whole M1 segment is replaced.

These results are consistent with previous findings by SCAM assay in which two cysteine reactive sites on equivalent positions on Cx46 and (I34 and L35) Cx32E<sub>1</sub>43 (I33 and M34) yielded the strongest inhibition when thiol reagent was applied. These two positions were on the extracellular half of M1 segment.

### Transfer of single-channel conductance in response to domain swapping between Cx46 and Cx37

To test whether conductance exchange is a phenomenon specific for Cx46 and Cx32E<sub>1</sub>43, we extended domain

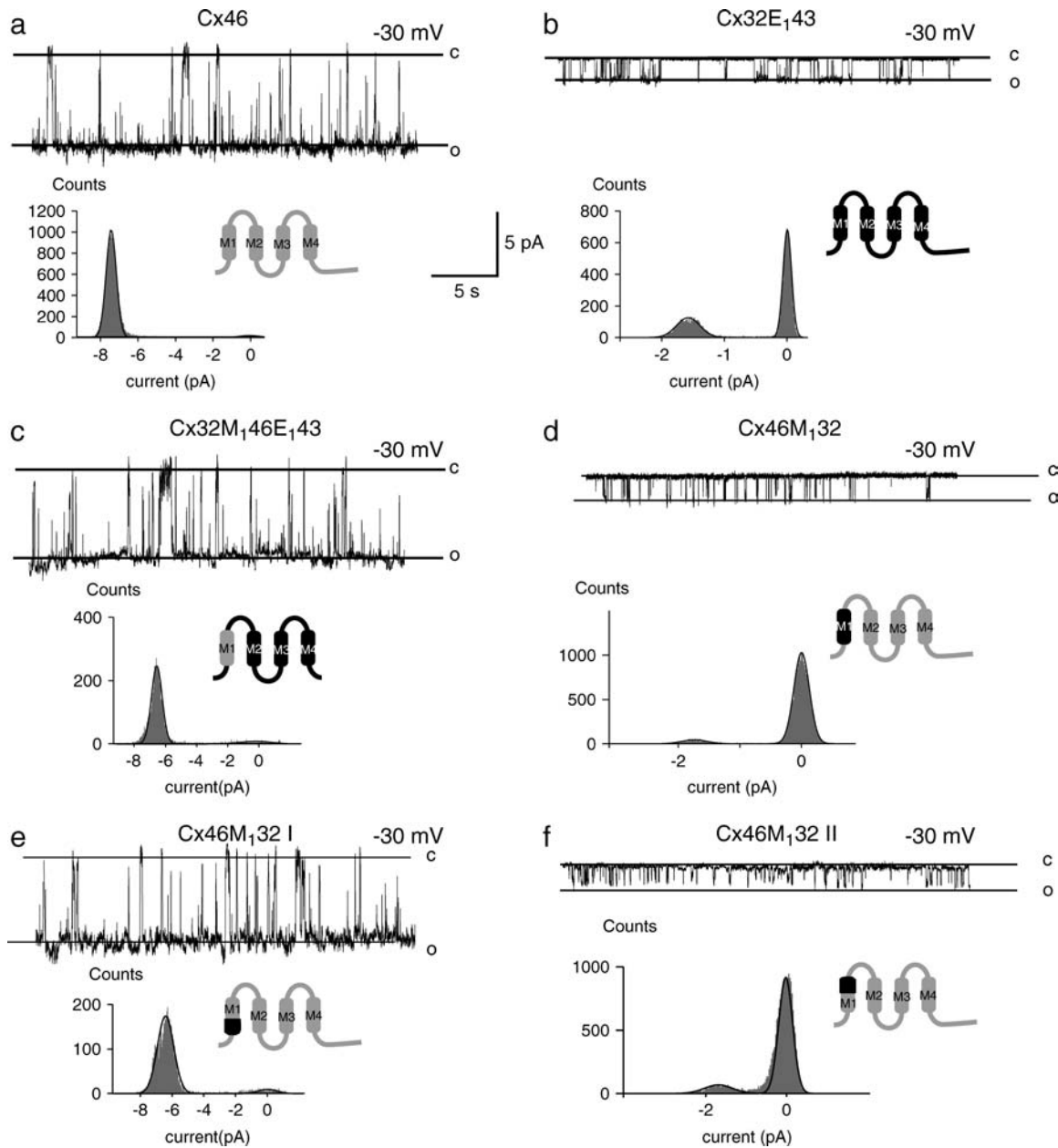


FIGURE 3 Single-channel currents recorded from inside-out patches that were excised from oocytes expressing Cx46, Cx32E<sub>1</sub>43, Cx32M<sub>1</sub>46 E<sub>1</sub>43, Cx46M<sub>1</sub>32, Cx46M<sub>1</sub>32I, and Cx46M<sub>1</sub>32II. Channels were held at negative potentials. Corresponding all-point amplitude histograms are shown under each current trace. Open (o) and close (c) states are indicated by dotted lines.

exchange to another connexin channel, Cx37. Sequence alignment of M1 identifies a three-amino-acids difference between Cx46 and Cx37 (Fig. 2), all of which are located at the extracellular half of M1. Cx37 forms gap junction channels with the largest known conductance of 300 pS (35). We generated another chimera, where the M1 in Cx46 was replaced with that of Cx37. The chimera Cx46M<sub>1</sub>37 opened as hemichannel in whole-cell experiments. Oocytes injected with the chimera mRNA showed increased membrane conductance that was voltage dependent. It has been shown

that the channel conductance of complete Cx46 gap junction channels is half the conductance of the Cx46 hemichannels, as if the complete gap junction channel are composed of two hemichannels in series without docking affecting channel conductance (36). If the same rule applies to Cx37, one would expect the single-channel conductance of chimera Cx46M<sub>1</sub>37 to be ~600 pS.

Single-channel conductance of Cx46M<sub>1</sub>37 was 520 pS at -30 mV and 300 pS at +24 mV (Fig. 5), which was close to the predicted Cx37 conductance and much larger than that

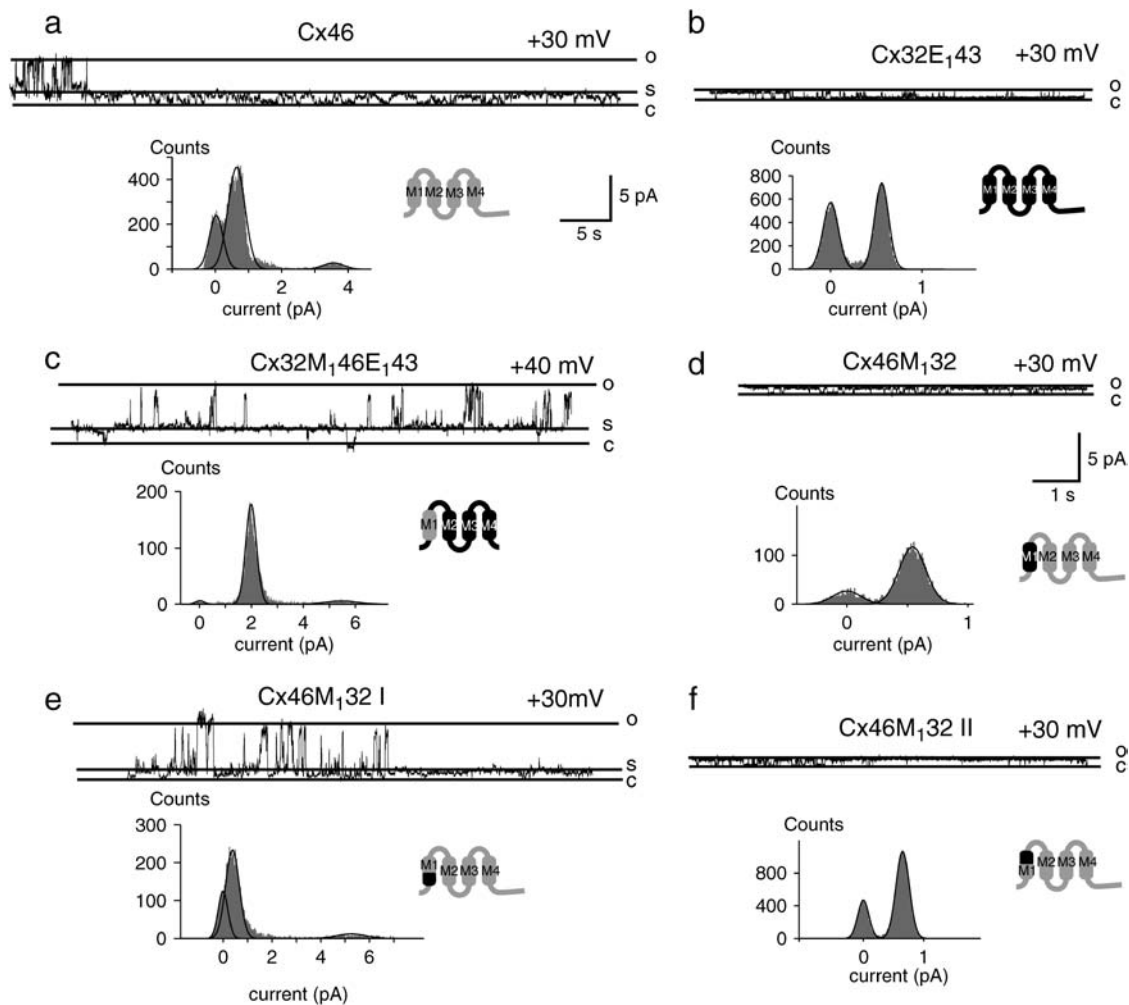


FIGURE 4 Single-channel currents recorded from inside-out patches that were excised from oocytes expressing Cx46, Cx32E<sub>143</sub>, Cx32M<sub>146</sub>E<sub>143</sub>, Cx46M<sub>132</sub>, Cx46M<sub>132</sub>I, and Cx46M<sub>132</sub>II. Channels were held at positive potentials. Corresponding all-point amplitude histograms are shown under each current trace. Open (o), close (c), and subconductance (s) states are indicated by dotted lines.

of Cx46. Cx46M<sub>137</sub> also exhibited a subconductance state at positive potentials as shown in Fig. 5 c, but this phenomenon appeared not as prominent as in Cx46.

The presented results show that M1, specifically the extracellular half of M1, determines the unitary conductances of Cx32, Cx37, and Cx46 channels. These conductances are summarized in Table 1.

### Single amino acid mutation of leucine at 35 position in Cx46

In an effort to further narrowing down critical pore lining structure we constructed the Cx46L35G mutant in which leucine at position 35 was replaced by glycine, the amino acid with the smallest side chain. The reason we chose this residue was based on observations from SCAM assay. It was shown that the cysteine mutation at position 35 in Cx46 as well as 34 position in Cx32E<sub>143</sub>, which were at equivalent

position on M1, caused the largest inhibition effect on single-channel conductance when thiol reagent was applied (21).

The unitary conductance was significantly increased in the Cx46L35G mutant as compared to wild-type (wt) Cx46. In symmetrical 140 mM potassium gluconate solution it was 377 pS for Cx46L35G and 312 pS for Cx46 (Fig. 6, g and h; Table 2). In KCl solution, the single-channel conductance was 489 pS for Cx46L35G and 359 pS for Cx46 wild type (Table 2).

Channel permeability to potassium<sup>+</sup>, chloride<sup>-</sup>, and gluconate<sup>-</sup> ion based on reversal potentials revealed insignificant differences between Cx46 and Cx46L35G (Fig. 6; Table 2). The reversal potentials for KGlu were +27 mV for Cx46 and +32 mV for Cx46L35G. The reversal potentials for KCl were +50 mV for Cx46 and +51 mV for Cx46L35G. Based on the Goldman-Hodgkin-Katz equation, the calculated permeability ratio of K<sup>+</sup>/Cl<sup>-</sup> was 21:1 in Cx46 and 25:1 in Cx46L35G. The permeability ratio of K<sup>+</sup>/Glu<sup>-</sup>

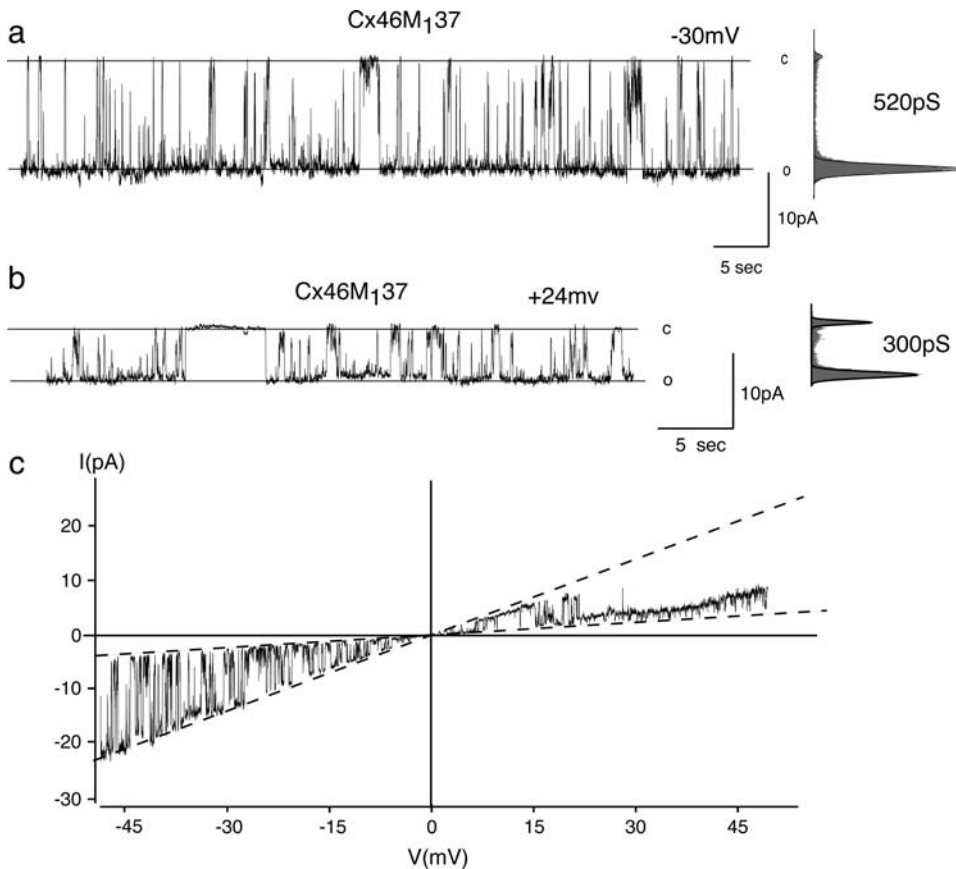


FIGURE 5 Single-channel currents in membrane patches excised from oocytes expressing Cx46M<sub>137</sub> at negative (a) potential, positive (b) potential, and during voltage ramps from +50 to -50 mV (c). All-point amplitude histograms and single-channel conductance at negative and positive potentials are shown beside the corresponding current traces.

was 4:1 in Cx46 and 5:1 in Cx46L35G. The calculated permeation ratio of  $\text{Glu}^-/\text{Cl}^-$  was 5:1 in both Cx46 and Cx46L35G.

These data would suggest that gluconate was more permeable than chloride. However, the chord conductance in the presence of the two anions shows otherwise. The channel conductance in KCl solution was significantly higher than in K<sub>2</sub>Glu solution (Fig. 6, *g* and *h*; Table 2).

### Spermine permeates 46L35G and Cx46M137 channels, but not wild-type Cx46 channels

As shown above, the single-channel conductance of two Cx46 mutants, Cx46M<sub>137</sub> and Cx46L35G, was much larger than the wild-type Cx46. As a preliminary attempt to test whether the pore of these two mutants was also enlarged, the large positively charged spermine ion was used in single-channel recording. Endogenous spermine was found to cause block and modulation of several types of ion channels by plugging the pore of the channel. For example, intracellular spermine was found responsible for rectification of inward rectifier  $\text{K}^+$  channel and some subtypes of  $\text{Ca}^{2+}$  permeable glutamate receptors (37).

As shown in Fig. 7, permeation differences between Cx46 wild type and mutants were observed when spermine

tetrahydrochloride chloride was used. With 15 mM spermine tetrahydrochloride chloride inside the pipette, 150 mM spermine tetrahydrochloride chloride solution was perfused to the inside-out patches containing the designated connexin channel. The reversal potential of Cx46 was near -60 mV (Fig. 7 *a*), which was close to the reversal potential of the chloride ion. Thus, Cx46 was impermeable to spermine. The reversal potential for Cx46L35G was  $\sim -10$  mV (Fig. 7 *b*), which meant spermine was permeable to the Cx46L35G channel though less permeant than the chloride ion. The reversal potential for Cx46M<sub>137</sub> in spermine tetrahydrochloride chloride solution was  $\sim 30$  mV (Fig. 7 *c*), which meant spermine was also permeant in the Cx46M<sub>137</sub> channel.

## DISCUSSION

These data show that the first transmembrane segment, specifically its extracellular half, is a determinant of channel conductance. Reciprocal exchange of this segment between two connexins led to a transfer of the single-channel conductance from the M1 donor to the recipient connexin. In addition, replacement by the corresponding Cx37 sequence resulted in the large single-hemichannel conductance typical for Cx37. Finally, point mutation of L35 to the short

**TABLE 1 Comparison of unit conductance of wild-type connexins and the chimeras at negative potentials**

	$\gamma$ (pS)		$\gamma$ (pS)
Cx46	258 $\pm$ 37 (13)	Cx32E <sub>1</sub> 43	54 $\pm$ 5 (11)
Cx32M <sub>1</sub> 46 E <sub>1</sub> 43	236 $\pm$ 29 (9)	Cx46M <sub>1</sub> 32	51 $\pm$ 3 (8)
Cx46M <sub>1</sub> 32I	270 $\pm$ 18 (5)	Cx46M <sub>1</sub> 32II	40 $\pm$ 5 (5)
Cx46M <sub>1</sub> 37	440 $\pm$ 84 (9)*	–	–

Conductance is expressed as mean  $\pm$  SD (number of channels analyzed).

side-chain amino acid glycine created a channel with enhanced conductance.

Conductance of a channel is governed by steric constraints as well as by electrostatic factors. The steric constraints include length and width of the conduction pathway as in any conductor. The electrostatic factors include not only interactions of the permeant ions with the channel wall, but also the availability of permeant ions. For the large conductance potassium (BK) channel it has been shown, that a ring of negative charges at the channel mouth affect both conductance and rectification of the channel (38). A similar mechanism appears to apply to Cx46 hemichannels, where fixed charges in the first extracellular loop affect selectivity, conductance, and rectification of the channel (22). These charges are thought to increase the local concentration of cations at the channel entry and thus their availability for passage through the channel. In this context the effect of extracellular loop charges should be hemichannel specific, as these sites become located in the center of the complete gap junction channel after docking and thus could not concentrate cations as they do at the mouth of the hemichannel. For complete gap junction channels cytoplasmic surface charges instead have been proposed to exert a similar role (39).

Because the amino acids exchanged in this study do not contain charged amino acids, steric rather than electrostatic factors have to be considered for the observed changes in conductance. Whether the M1 domain represents a pore constriction or whether this sequence imposes structural constraints on adjacent or contacting domains cannot be derived from this data with certainty. The latter possibility has to be considered because the transfer of conductance appears to be context dependent. For example, if M1 is exchanged together with the amino terminus no functional channel is formed for Cx32E<sub>1</sub>43 as recipient (26,28). With Cx46 as recipient for the equivalent Cx32 sequence no change of conductance was observed (28).

Conductance and channel rectification were found to be affected by mutational alteration of negatively charged amino acids in the first extracellular loop as well as by charged methanethiosulfonate (MTS) reagents reacting with engineered cysteines in E1 (22,28). It thus appears that in the Cx46 hemichannel the E1 segment determines conductance based on electrostatic principles whereas the M1 segment imparts a steric hindrance for the transit of ions through the channel. The SCAM data already yielded some clues about

the molecular dimensions of the two domains. Reaction of engineered cysteines in E1 with MTS resulted in a stepwise reduction of single-channel conductance. Because six steps could be resolved this was interpreted as a successive reaction of MTS with all six subunits of the channel (22). Reaction of maleimidobutyryl-biocytyl (MBB) at position 35 in M1 on the other hand resulted in a one step,  $\sim$ 80% reduction of the single-channel conductance (23,40). Apparently the channel can accommodate only one MBB molecule at that position. Although MBB with a molecular mass of 537 Da is larger than the MTS molecules (233–278 Da), six MTS molecules occupy a considerably larger volume than a single MBB molecule. Based on these considerations the pore lining contributing M1 segment has a smaller pore dimension than the segment contributed by E1.

In the SCAM assays of Cx46 connexons (21,22,24) reactive cysteines were found only in the extracellular half of M1. The same segment also was found in this study to be sufficient for the transfer of channel conductance between connexins whereas the exchange of the amino-terminal half of M1 remained inconsequential. M1 thus is unlikely to provide all of the pore lining moieties in the transmembrane part of the channel. Based on the weak inhibition of Cx32E<sub>1</sub>43-induced membrane conductance by MBB, it was proposed (21) that M3 furnishes the remainder of the transmembrane portion of the pore in the form of a wider vestibulum. A combination M1/M3 pore has also been proposed based on crystallographic and phylogenetic data (24). However, single-channel SCAM on Cx46 showed only minimal inhibition of channel conductance in the M3 segment. Because the latter experiments were performed with the small MTS molecules, a significant reduction may not need to be expected in a wide part of the channel.

If the M1 segment were to represent the narrow part of the pore one would expect that the permeability and selectivity of the channel be affected by mutations in this segment. Although a detailed analysis of this aspect is presented in the accompanying article, reversal potential measurements indicate that at least the L35 position in Cx46 is critical in this respect. A cysteine in this position reacts with extracellularly and intracellularly applied thiol reagents (21–23). A change to glycine renders the channel permeable to spermine. Application of a spermine tetrahydrochloride chloride concentration gradient to a Cx46L35G channel in an excised patch resulted in a reversal potential considerably less negative than the chloride equilibrium potential. In wild-type channels the reversal potential instead was close to the chloride equilibrium potential under the same experimental conditions. Similarly, replacement of M1 with the corresponding Cx37 sequence resulted in spermine permeability.

It has been suggested that in some connexins, spermine induces a voltage-dependent channel block (41,42) akin to the rectification mechanism in inward rectifying potassium channels (37,41–45). Amino-terminal glutamate residues have been suggested to contribute to the spermine binding sites in

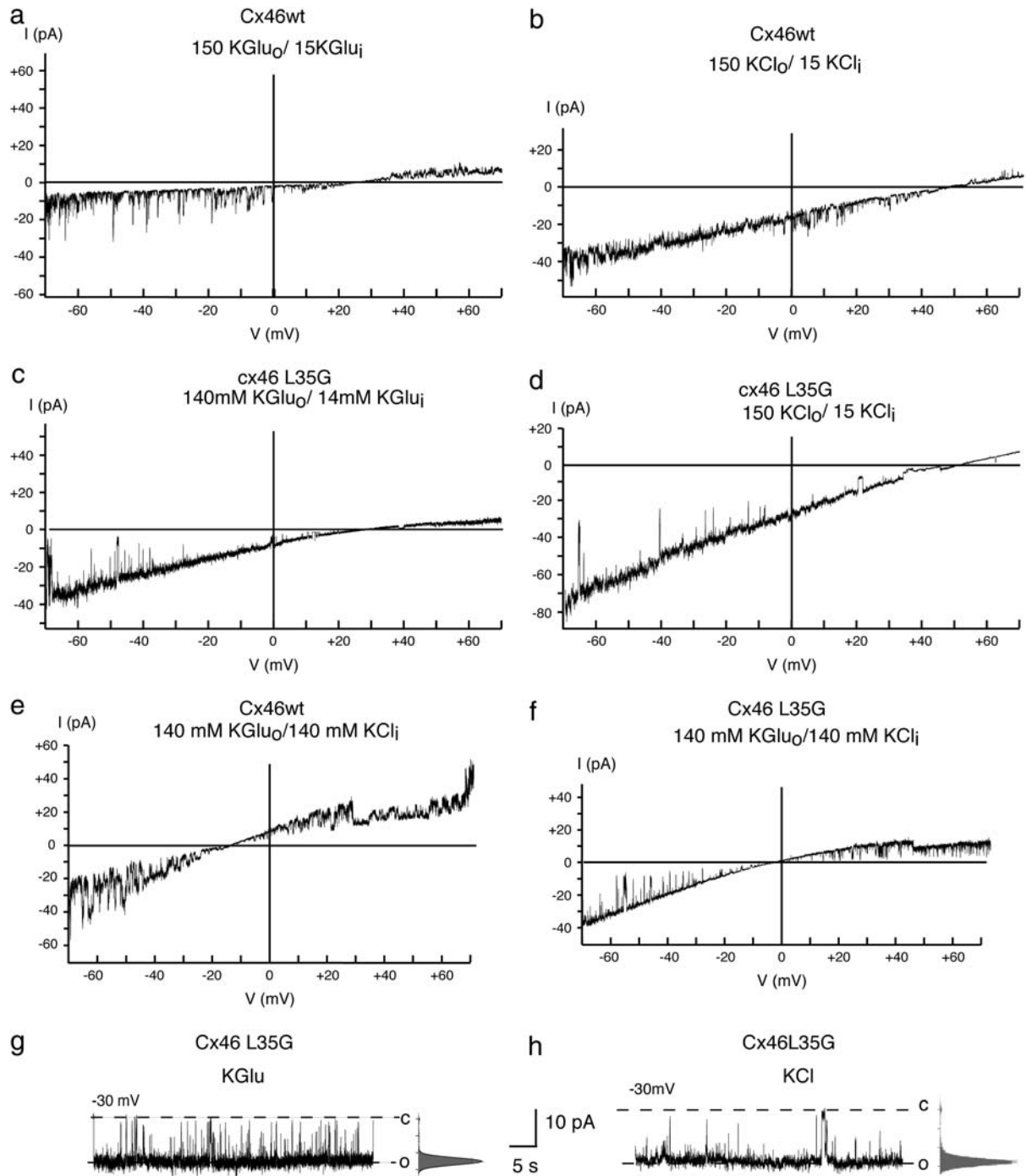


FIGURE 6 Voltage ramps of Cx46 (*a, b, e*) and Cx46L35G (*c, d, f*) channels contained in inside-out patches in 150 mM K<sub>Clu</sub> (pipette)/15 mM K<sub>Clu</sub> (bath) (*a, c*), 150 mM K<sub>Cl</sub> (pipette)/15 mM K<sub>Cl</sub> (bath) (*b, d*) salt gradients, and 140 mM K<sub>Clu</sub> (pipette)/140 mM K<sub>Cl</sub> (bath) bionic conditions (*e, f*). Single-channel currents at  $-30$  mV holding potential of Cx46L35G channels in symmetric K<sub>Clu</sub> (*g*) and K<sub>Cl</sub> (*h*), 150 mM each. In addition to the specified ions, all solutions also contained 5 mM TES, pH 7.5. No adjustment for osmolarity or ionic strength was performed.

Cx40 (42). Cx46 also has identically spaced glutamates in the amino-terminus. However, because neither the L to G change nor the M1 swap with the Cx37 sequence involve changes of charged amino acids, a direct electrostatic effect on putative binding sites can be ruled out.

Another indication that L35 imparts steric constraints on the channel comes from the observation that the L35G mutant has a higher exclusion limit for fluorescent tracers as compared to wild-type Cx46. Stachyose fluorescein (1146 mol wt) is excluded from oocytes expressing wt Cx46 but



**TABLE 2 Comparison of ion permeability between wild-type Cx46 and Cx46L35G**

$\gamma$ (pS)	Wild-type cx46	Cx46L35G
$\gamma_{\text{KGluc}}$	$312 \pm 10$ (8)	$377 \pm 5$ (7)
$\gamma_{\text{KCl}}$	$359 \pm 6$ (8)	$489 \pm 11$ (5)
$p_{\text{K/pGlu}}$	$4 \pm 1$ (4)	$5 \pm 1$ (3)
$p_{\text{K/pCl}}$	$21 \pm 2$ (4)	$25$ (2)
$p_{\text{Glu/pCl}}$	5	5

Single-channel conductance (pS) in 140 mM symmetric KGluc and KCl are listed in the first and second row, respectively. Permeability ( $p$ ) ratio of  $\text{K}^+/\text{Glu}^-$ ,  $\text{K}^+/\text{Cl}^-$ , and  $\text{Glu}^-/\text{Cl}^-$  are listed in the subsequent rows. Data are shown as mean  $\pm$  SD (number of channels analyzed).

appears in the cytoplasm of oocytes expressing Cx46L35G upon extracellular application of the fluorescent tracer (46).

The moderate cation selectivity of wild-type Cx46 channels (36) is present to a similar extent in the Cx46L35G mutant. Unexpectedly, in both wild-type and mutant channels the relative permeabilities of Cl and gluconate are reversed when

determined by chord conductance measurements as compared to determination by reversal potential measurement and calculation with the Goldman-Hodgkin-Katz equation (Table 1; Fig. 6). It is counterintuitive that the larger gluconate molecule should be more permeant than the smaller chloride. Both carry the same charge, excluding electrostatic factors. An apparently higher permeability for the larger glutamate over chloride was also noted before for Cx40 gap junction channels (47). However, in contrast to discrepancy between chord conductance and reversal potential measurements observed in this study no such incongruity was found for the Cx40 channel. Whatever the mechanism, it appears that the L35G mutation affects conductance of the channel without changing selectivity.

Besides modifying conductance, the M1 exchange also resulted in a transfer of some voltage gating properties from the donor connexin to the recipient. The exchange did not involve charged residues that per se could have carried voltage-dependent behaviors. It appears that the M1 instead

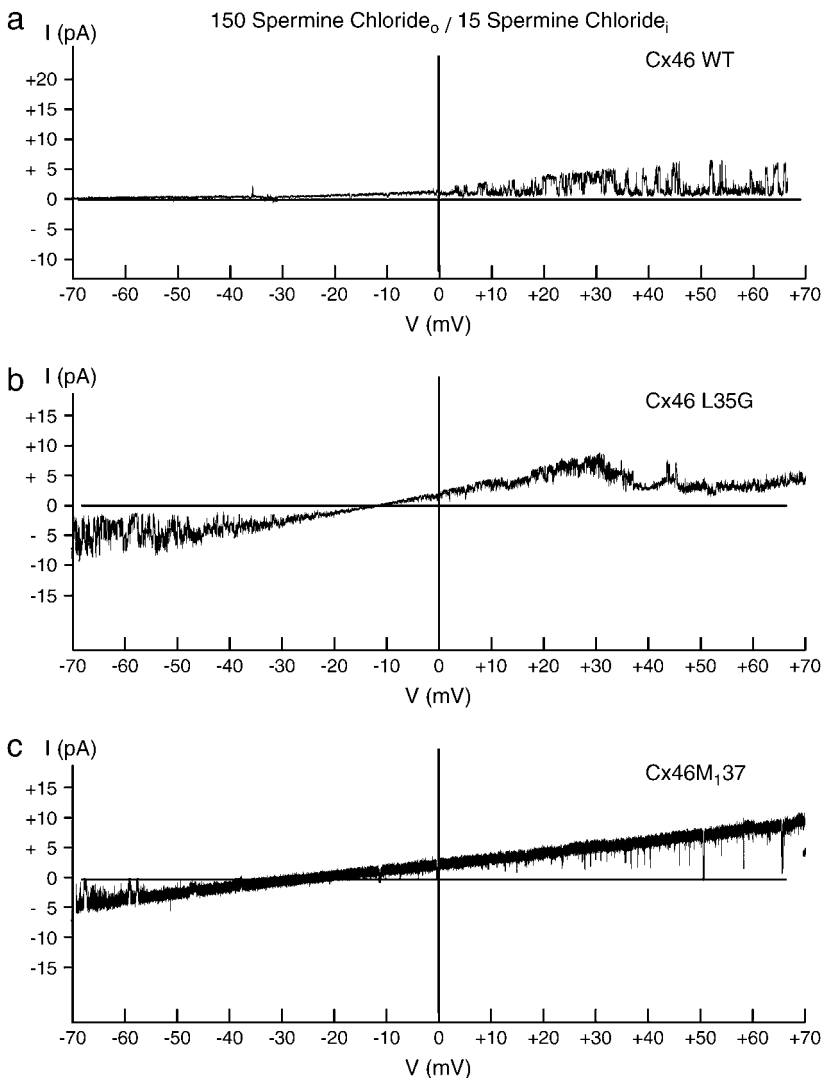


FIGURE 7 Voltage ramps of wide-type Cx46 (a), Cx46L35G (b), and Cx46M<sub>1,37</sub> (c) channel contained in an inside-out patch in the presence of the 150-mM (pipette)/10-mM (bath) spermine tetrahydrochloride gradient.

is capable of translating voltage-dependent events originating in other parts of the channel into M1-specific variations of conductance.

As relating to the discrepancy between the different SCAM studies on hemichannels and complete gap junction channels this could be caused by a number of reasons. There could be a difference between the pore linings of channels formed by different connexins, there may be differences between hemichannels and complete gap junction channels, or the different methods employed in the three studies may give different results. The data on Cx32 gap junction channels were exclusively based on macroscopic current effects where the thiol reagent was applied to the cytoplasmic side with the necessity to penetrate a thick layer of yolk and all the reductive capacity of the cytoplasm. Nicholson and co-workers (25) found that certain sites could be reacted with the thiol reagent applied extracellularly, a constellation where the reagent should have no access to the pore of the complete gap junction channel. This was interpreted as evidence for large crevices in the channel wall accessible from the extracellular space. An alternative interpretation, however, has to be considered. Gap junctions in oocytes as in other cells are very dynamic. They turn over rapidly with a half-life of 1–2 h. In oocytes the formation rate exceeds degradation to an extent that even within the typical exposure time to the thiol reagent junctional conductance in an oocyte pair increases appreciably (25). Thus, the thiol reagent could get access to the pore during the docking process without the need of crevices contiguous with the extracellular space.

## SUPPLEMENTARY MATERIAL

An online supplement to this article can be found by visiting BJ Online at <http://www.biophysj.org>.

We thank Drs. C. Grewer and W. Nonner for valuable discussions and for critically reading the manuscript.

This work was supported by the National Institutes of Health (grant GM48610).

## REFERENCES

- Evans, W. H., and P. E. Martin. 2002. Gap junctions: structure and function (review). *Mol. Membr. Biol.* 19:121–136.
- Harris, A. L. 2001. Emerging issues of connexin channels: biophysics fills the gap. *Q. Rev. Biophys.* 34:325–472.
- Bruzzone, R., S. G. Hormuzdi, M. T. Barbe, A. Herb, and H. Monyer. 2003. Pannexins, a family of gap junction proteins expressed in brain. *Proc. Natl. Acad. Sci. USA.* 100:13644–13649.
- Panchin, Y., I. Kelmanson, M. Matz, K. Lukyanov, N. Usman, and S. Lukyanov. 2000. A ubiquitous family of putative gap junction molecules. *Curr. Biol.* 10:473–474.
- Sohl, G., and K. Willecke. 2004. Gap junctions and the connexin protein family. *Cardiovasc. Res.* 62:228–232.
- Baranova, A., D. Ivanov, N. Petrash, A. Pestova, M. Skoblov, I. Kelmanson, D. Shagin, S. Nazarenko, E. Geraymovych, O. Litvin, A. Tiunova, T. L. Born, et al. 2004. The mammalian pannexin family is homologous to the invertebrate innexin gap junction proteins. *Genomics.* 83:706–716.
- Goodenough, D. A., and D. L. Paul. 2003. Beyond the gap: functions of unpaired connexon channels. *Nat. Rev. Mol. Cell Biol.* 4:285–294.
- Bukauskas, F. F., and V. K. Verselis. 2004. Gap junction channel gating. *Biochim. Biophys. Acta.* 1662:42–60.
- Plum, A., G. Hallas, T. Magin, F. Dombrowski, A. Hagendorff, B. Schumacher, C. Wolpert, J. Kim, W. H. Lamers, M. Evert, P. Meda, O. Traub, et al. 2000. Unique and shared functions of different connexins in mice. *Curr. Biol.* 10:1083–1091.
- Paul, D. L., L. Ebihara, L. J. Takemoto, K. I. Swenson, and D. A. Goodenough. 1991. Connexin46, a novel lens gap junction protein, induces voltage-gated currents in nonjunctional plasma membrane of *Xenopus* oocytes. *J. Cell Biol.* 115:1077–1089.
- Pfahnl, A., X. W. Zhou, R. Werner, and G. Dahl. 1997. A chimeric connexin forming gap junction hemichannels. *Pflugers Arch.* 433:773–779.
- Beahm, D. L., and J. E. Hall. 2002. Hemichannel and junctional properties of connexin 50. *Biophys. J.* 82:2016–2031.
- Hofer, A., and R. Dermietzel. 1998. Visualization and functional blocking of gap junction hemichannels (connexons) with antibodies against external loop domains in astrocytes. *Glia.* 24:141–154.
- DeVries, S. H., and E. A. Schwartz. 1992. Hemi-gap-junction channels in solitary horizontal cells of the catfish retina. *J. Physiol.* 445:201–230.
- Kondo, R. P., S. Y. Wang, S. A. John, J. N. Weiss, and J. I. Goldhaber. 2000. Metabolic inhibition activates a non-selective current through connexin hemichannels in isolated ventricular myocytes. *J. Mol. Cell. Cardiol.* 32:1859–1872.
- Ebihara, L., and E. Steiner. 1993. Properties of a nonjunctional current expressed from a rat connexin46 cDNA in *Xenopus* oocytes. *J. Gen. Physiol.* 102:59–74.
- Verselis, V. K., E. B. Trexler, and F. F. Bukauskas. 2000. Connexin hemichannels and cell-cell channels: comparison of properties. *Braz. J. Med. Biol. Res.* 33:379–389.
- Ebihara, L., V. M. Berthoud, and E. C. Beyer. 1995. Distinct behavior of connexin56 and connexin46 gap junctional channels can be predicted from the behavior of their hemi-gap-junctional channels. *Biophys. J.* 68:1796–1803.
- Trexler, E. B., F. F. Bukauskas, M. V. Bennett, T. A. Bargiello, and V. K. Verselis. 1999. Rapid and direct effects of pH on connexins revealed by the connexin46 hemichannel preparation. *J. Gen. Physiol.* 113:721–742.
- Akabas, M. H., C. Kaufmann, P. Archdeacon, and A. Karlin. 1994. Identification of acetylcholine receptor channel-lining residues in the entire M2 segment of the alpha subunit. *Neuron.* 13:919–927.
- Zhou, X. W., A. Pfahnl, R. Werner, A. Hudder, A. Llanes, A. Luebke, and G. Dahl. 1997. Identification of a pore lining segment in gap junction hemichannels. *Biophys. J.* 72:1946–1953.
- Kronengold, J., E. B. Trexler, F. F. Bukauskas, T. A. Bargiello, and V. K. Verselis. 2003. Single-channel SCAM identifies pore-lining residues in the first extracellular loop and first transmembrane domains of Cx46 hemichannels. *J. Gen. Physiol.* 122:389–405.
- Pfahnl, A., and G. Dahl. 1998. Localization of a voltage gate in connexin46 gap junction hemichannels. *Biophys. J.* 75:2323–2331.
- Fleishman, S. J., V. M. Unger, M. Yeager, and N. Ben-Tal. 2004. A Calpha model for the transmembrane alpha helices of gap junction intercellular channels. *Mol. Cell.* 15:879–888.
- Skerrett, I. M., J. Aronowitz, J. H. Shin, G. Cymes, E. Kasperek, F. L. Cao, and B. J. Nicholson. 2002. Identification of amino acid residues lining the pore of a gap junction channel. *J. Cell Biol.* 159:349–360.
- Hu, X., and G. Dahl. 1999. Exchange of conductance and gating properties between gap junction hemichannels. *FEBS Lett.* 451:113–117.
- Hartmann, H. A., G. E. Kirsch, J. A. Drewe, M. Tagliatela, R. H. Joho, and A. M. Brown. 1991. Exchange of conduction pathways between two related K<sup>+</sup> channels. *Science.* 251:942–944.

28. Trexler, E. B., F. F. Bukauskas, J. Kronengold, T. A. Bargiello, and V. K. Verselis. 2000. The first extracellular loop domain is a major determinant of charge selectivity in connexin46 channels. *Biophys. J.* 79:3036–3051.
29. Villmann, C., N. Strutz, T. Morth, and M. Hollmann. 1999. Investigation by ion channel domain transplantation of rat glutamate receptor subunits, orphan receptors and a putative NMDA receptor subunit. *Eur. J. Neurosci.* 11:1765–1778.
30. Ji, H. L., L. R. Bishop, S. J. Anderson, C. M. Fuller, and D. J. Benos. 2004. The role of Pre-H2 domains of alpha- and delta-epithelial Na<sup>+</sup> channels in ion permeation, conductance, and amiloride sensitivity. *J. Biol. Chem.* 279:8428–8440.
31. Fishman, G. I., A. P. Moreno, D. C. Spray, and L. A. Levin. 1991. Functional analysis of human cardiac gap junction channel mutants. *Proc. Natl. Acad. Sci. USA.* 88:3525–3529.
32. Manthey, D., K. Banach, T. Desplantez, C. G. Lee, C. A. Kozak, O. Traub, R. Weingart, and K. Willecke. 2001. Intracellular domains of mouse connexin26 and -30 affect diffusional and electrical properties of gap junction channels. *J. Membr. Biol.* 181:137–148.
33. Dahl, G. 1992. The *Xenopus* oocyte cell-cell channel assay for functional analysis of gap junction proteins. In *Cell-cell Interactions. A Practical Approach*. B. Stevenson, W. Gallin, and D. Paul, editors. IRL, Oxford, UK. 143–165.
34. Hamill, O. P., A. Marty, E. Neher, B. Sakmann, and F. J. Sigworth. 1981. Improved patch-clamp techniques for high-resolution current recording from cells and cell-free membrane patches. *Pflügers Arch.* 391:85–100.
35. Veenstra, R. D., H. Z. Wang, E. C. Beyer, S. V. Ramanan, and P. R. Brink. 1994. Connexin37 forms high conductance gap junction channels with subconductance state activity and selective dye and ionic permeabilities. *Biophys. J.* 66:1915–1928.
36. Trexler, E. B., M. V. Bennett, T. A. Bargiello, and V. K. Verselis. 1996. Voltage gating and permeation in a gap junction hemichannel. *Proc. Natl. Acad. Sci. USA.* 93:5836–5841.
37. Williams, K. 1997. Interactions of polyamines with ion channels. *Biochem. J.* 325:289–297.
38. Brelidze, T. I., X. Niu, and K. L. Magleby. 2003. A ring of eight conserved negatively charged amino acids doubles the conductance of BK channels and prevents inward rectification. *Proc. Natl. Acad. Sci. USA.* 100:9017–9022.
39. Banach, K., S. V. Ramanan, and P. R. Brink. 2000. The influence of surface charges on the conductance of the human connexin37 gap junction channel. *Biophys. J.* 78:752–760.
40. Dahl, G., and A. Pfahnl. 2001. Mutagenesis to study channel structure. *Methods Mol. Biol.* 154:251–268.
41. Musa, H., and R. D. Veenstra. 2003. Voltage-dependent blockade of connexin40 gap junctions by spermine. *Biophys. J.* 84:205–219.
42. Musa, H., E. Fenn, M. Crye, J. Gemel, E. C. Beyer, and R. D. Veenstra. 2004. Amino terminal glutamate residues confer spermine sensitivity and affect voltage gating and channel conductance of rat connexin40 gap junctions. *J. Physiol.* 557:863–878.
43. Lopatin, A. N., E. N. Makhina, and C. G. Nichols. 1995. The mechanism of inward rectification of potassium channels: “long-pore plugging” by cytoplasmic polyamines. *J. Gen. Physiol.* 106:923–955.
44. Shyng, S. L., Q. Sha, T. Ferrigni, A. N. Lopatin, and C. G. Nichols. 1996. Depletion of intracellular polyamines relieves inward rectification of potassium channels. *Proc. Natl. Acad. Sci. USA.* 93:12014–12019.
45. Williams, K. 1997. Modulation and block of ion channels: a new biology of polyamines. *Cell. Signal.* 9:1–13.
46. Hu, X. A study of the pore of gap junction hemichannels. 2001. PhD thesis. University of Miami, Miami, FL.
47. Beblo, D. A., and R. D. Veenstra. 1997. Monovalent cation permeation through the connexin40 gap junction channel. Cs, Rb, K, Na, Li, TEA, TMA, TBA, and effects of anions Br, Cl, F, acetate, aspartate, glutamate, and NO<sub>3</sub>. *J. Gen. Physiol.* 109:509–522.